Deep Learning Based Power Allocation for Workload Driven Full-Duplex D2D-Aided Underlaying Networks

Changhao Du [ID], Zhongshan Zhang [ID], *Senior Member, IEEE*, Xiaoxiang Wang, and Jianping An [ID], *Member, IEEE*

Abstract—Both Device-to-device (D2D) and full-duplex (FD) have been widely recognized as spectrum efficient techniques in the fifth-generation (5G) networks. By combining them, the FD-D2D aided underlaying networks (FN) has exhibited considerable technical advantages in terms of both spectral efficiency (SE) and energy efficiency (EE). Considering the fact that the performance of FN may be severely affected by users' workload, the workload-driven FN (WFN) must be investigated. In this paper, a deep learning based transmit power allocation (TPA) method is proposed for automatically determining the optimal transmit powers of co-spectrum cellular users (CUs) and D2D users (DUs) relying on a deep neural network. Unlike the conventional transmit-power-control schemes, in which complex optimization problems must be addressed in an iterative manner (it usually requires a relative longer computational time), the proposed scheme enables each DU to determine its transmit power with a relatively shorter time. Furthermore, an improved iterative subspace-pursuit algorithm, as the performance benchmark, is formulated for WFN. In addition, to reflect the influence imposed by the workload, the penalty-based statistical sum-date-rate (PSS) can be employed as the performance metric of WFN. Numerical results show that the proposed scheme is capable of achieving a PSS comparable with that of the traditional iterative-based algorithms even under heavy-workload scenarios, but the computational complexity of the former can be significantly reduced.

Index Terms—Deep neuron network, device-to-device, full-duplex, underlaying cellular networks, activated probability.

I. INTRODUCTION

WITH the rapid development as well as the increasing commercialization progress of the fifth-generation (5G) communication technology, new services (such as video on demand) are emerging quickly, resulting in an explosive increase in network's workload. This trend poses serious challenges to the utilization of network resources and the improvement of network throughput [1]–[5]. Furthermore, under the conventional base station (BS)-centric cellular network architecture, the BS may often operate at an overloaded state (especially in a rush hour), thus resulting in a severe load imbalance over the network [6].

The Device-to-device (D2D) technology, which allows the close-by devices to communicate directly without relying on the involvement of BSs, has been regarded as one of the critical techniques for the 5G systems to provide an unprecedented quality of service (QoS) to the customers [7], [8]. Several advantages, including a significantly improved throughput [9], an increased spectral efficiency [10], [11], an extended radio coverage [12], a reduced power consumption in mobile devices [13], [14], and an efficaciously relieved traffic budget at the BS [15], etc, have been exhibited in D2D technology. In addition to D2D technology, the full-duplex (FD) is also regarded as one of the core technologies of 5G systems. Since the FD devices are allowed to concurrently transmit and receive signal over a single spectrum, the spectral efficiency (SE) of the cellular networks (CN) can be doubled as compared to the traditional half-duplex (HD) technology [16]–[18]. On this basis, if we can combine both FD and D2D (that is, to form a new technology called FD-D2D) and give full play to their advantages, the SE of CN will inevitably be further improved.

Although FD-D2D technique is capable of tremendously improving the SE, it also imposes extra interference on CN due to the increased density of users, which may share the same set of radio resources in the FD-D2D aided underlaying networks (FN). Therefore, it is crucial to perform transmit power allocation (TPA) in FD-D2D devices. Once an improper TPA is implemented, it is very likely to cause an interference strong enough to run out of control, resulting in a fall back of the performance of CN [19], [20].

A. Motivation

Although TPA for D2D-aided underlaying networks (DN) has received a wide attention by both academia and industry, its implementation in FN is still to be investigated. In particular, the following challenges must be addressed:

1) The impact of workload: Whether to activate a user or not depends on the user's workload. When the traffic load

of users becomes heavier, the wireless spectrum must be shared among users in order to improve its utilization. However, this kind of spectrum sharing will inevitably lead to an excessive traffic load on an individual spectrum. The high workload will definitely cause a strong interference among co-spectrum users, (very likely) causing a transmission failure. Therefore, FN faces enormous challenges in terms of interference suppression/mitigation [21].

2) The impact of severe self-interference (SI): The SI between the transmit and receive antennas of each FD device may significantly drown out the signal of interest that was transmitted by a remote transmitter [22]. Although most of the SI power can be sufficiently suppressed by employing an appropriate SI cancellation (SIC) technique (please refer to [16] for details), the residual SI (RSI) power may still be high enough to erode the FD gains.

3) The impact of complicated mutual-interference (MI): On the one hand, in scenarios that DTs reuse the spectrum allocated to the traditional cellular users (CUs), the latter's performance will be seriously degraded. On the other hand, interference between DUs will also lead to a decrease in DU performance. In traditional HD-mode, only one pair of DUs can communicate at a time (other DUs remain silent), which can minimize interference between DUs. Unlike HD-mode, more serious MI happens among FD-mode DUs. Therefore, FD-D2D must cope with more complicated interference environments.

Generally speaking, TPA plays a vital role in suppressing interference between users in FN. If an improper TPA technology is employed, it will cause a serious erosion in FD-D2D performance. However, several important challenges, such as the impact of workload, the severe SI as well as the MI of FD-mode DUs, etc, must be solved when designing TPA algorithms for FN.

B. The Existing Work

Given that TPA plays a vital role in D2D communication [23], it has received a wide attention in both academia and industry [24], [25]. In the existed researches, there are mainly two categories for TPA, i.e., the iterative and deep learning algorithms.

1) The Iterative Algorithms: Most of the existing TPA studies were focused on solving the cost function, for which a sub-optimal solution relying on iterative algorithms is usually adopted for optimizing the transmission power, whenever the optimal solution in a closed-form cannot be pushed out. It has been demonstrated that a satisfactory performance can be obtained in most of iterative schemes. However, sufficient iterations are required in these algorithms, causing a relatively higher computational cost. Therefore, the iterative schemes may prevent the real-time operations that are essential in real systems. For instance, the iterative water-filling algorithm (IWA) proposed in [26] was based on the concept of competitive optimality, which involves singular value decomposition (SVD) at each iteration that requires a high computational cost. Furthermore, in [27], the interference pricing algorithms (IPA) were proposed,

in which the IPA iterations also require the SVD process and consume excessive computational resources. Moreover, semi-definite relaxation based scheme [28] lifts the original vector-based optimization problems into matrix-based problems, followed by solving one or more semi-definite programs that require high computational complexities. In particular, a typical subspace pursuit algorithm named weighted minimum mean squared error (WMMSE) was proposed in [29], which requires complex operations such as matrix inversion and bisection in each iteration. In addition, in some recent proposed iterative algorithms [30]–[33], the computational time still does not meet the real-time demand of practical systems.

Based on the existed studies, the computationally demanding nature of these algorithms imposes a big challenge on real-time implementation, because algorithms for a lot of applications (such as wireless transceiver design) are typically executed in a time frame of milliseconds. As the number of users increases, the scenario becomes severer, because more iterations are required [25]. To address the this issue, deep learning based power control scheme was proposed and attracted a wide attention.

2) Deep Learning Based Algorithms: Deep learning technology, which is based on deep neural network (DNN), has gained in popularity over the last decade due to its superior performance over the conventional techniques [34]–[40]. It is possible for us to solve complex non-linear problems in an efficient manner by using a back-propagation (BP) algorithm [41], in which a trained DNN model can be employed for reducing the computational time required in practical systems [37].

By employing deep learning technology, the performance of power control can be substantially improved. For instance, in [41], [42], a dense net-based transmit power control was proposed, in which the output of WMMSE based transmit power control strategy was regenerated for relieving the computational complexity of the WMMSE-based schemes. However, given that the main goal in this case was the regeneration of a WMMSE-based scheme, the DNN-based scheme cannot outperform the WMMSE-based scheme in terms of the achievable capacity. In [43], the weighted sum rate (WSR) of DUs can be maximized by employing DNN. Furthermore, in [44], the deep learning based ensemble power control network was proposed, in which several DNN models were combined together to achieve better performance. However, More computational resources than the basic deep learning algorithms are required in [44]. In addition, unlike the existing algorithms, a distributed power allocation method employing deep learning technique was proposed for D2D-aided underlaying long-term evolution (LTE) systems [45], which relied on the iterative-based prediction process.

Despite all this, there are still many deficiencies in the exiting deep learning based-power-control schemes. Firstly, in the existing heterogeneous systems comprising both DUs and CUs, the interference and channel gain among users were not properly analyzed. Secondly, without employing FD technology, the impact of RSI power on the system's performance was definitely ignored. Finally and most importantly, the impact of workload on the network's performance was not considered. In fact, the intensity of workload determines how frequently the user can be activated.

In this paper, a new transmit-power-control scheme employing deep learning technique is proposed for the workload-driven FN (WFN). The innovations and contributions of this paper are summarized as follows.

C. The Proposed Technological Approaches

To improve the performance gain (i.e., sum data rate) of the WFN, an appropriate power allocation technique may constitute a major concern, because a poorly controlled transmit power in CUs/DUs will definitely generate a strong interference that severely erodes the SE of the system. When we design power control algorithms, the following three aspects must be given special attention.

1) Excessively strong transmit power in a device will impose a strong interference on its co-spectrum devices, which consequently induces a performance loss in the WFN.
2) Generally speaking, a heavier workload on a licensed spectrum (it may be shared by several CUs and DUs) will lead to a stronger interference among these co-spectrum users. On this basis, the designed algorithm will inevitably obtain a higher performance gain by considering the state of each user (i.e., active or not).
3) When designing power control algorithms, special attention must be paid to the SI induced by activated FD-DUs. Basically, In the case of navigation, the higher the transmission power, the severer the RSI.

In summary, the transmit power of each user in the WFN must be well controlled according to both its current workload and the interference imposed on it.

D. Main Contributions

In this paper, a deep learning based TPA scheme is proposed, which is constructed following the deep neural network (DNN) by taking the impact of users' workload into account. Without loss of generality, a set of users (i.e., comprising N_c CUs and N_d D2D pairs) are allowed to share the same spectrum according to a non-homogeneous Poisson Point Processes (PPP) model. The main contributions of this paper are summarized in the following aspects:

1) A new system model is proposed for WFN by introducing the concept "penalty," which reflects the distortion caused by unsuccessful data transmissions. More importantly, we have fully considered the impact of users' workload on their activated probability (AP) in the proposed model.
2) According to the theory of subspace-pursuit (SP) based WMMSE algorithm, a workload-driven improved-iterative subspace-pursuit algorithm (WIS), which can be used as the performance benchmark, is proposed.
3) A deep TPA strategy for WFN, relying on DNN, is elaborated on in the proposed model, in which the transmit power for maximizing the penalty-based statistical sum-data-rate (PSS) of the WFN is derived by implementing the proposed deep learning scheme. Numerical results show that the performance of the proposed scheme is very closed to WIS, significantly outperforming the existing TPA schemes such as the conventional equal transmit

power (ETP) scheme and randomly transmit power (RTP) scheme in terms of the PSS.

The remainder of this paper is organized as follows. In Section II, the system model for the proposed WFN is described. The received SINRs for both CUs and DUs are analyzed in Section III, respectively. After that, the PSS of the WFN is evaluated in Section IV. Furthermore, the formulation of WIS is described in Section V, followed by giving out the optimization problem as well as detailed explanation on the proposed DNN-based TPA scheme in Section VI. In addition, numerical results are provided in Section VII. Finally, Section VIII concludes this paper.

Notation: $\mathbb{P}$ represents the probability of an event, and $\mathcal{P}$ denotes the transmit or receive power of a user. Meanwhile, $\mathcal{R}$ and I stand for the data rate and the MI, respectively. Furthermore, $\mathbb{E}$ is used to denote the expectation operation. In addition, the bold symbols are used to denote the matrix and/or vectors. Finally, $\lfloor \bullet \rfloor$ represents a round-down function. A list of symbols that employed in this paper is given by Table I.

II. SYSTEM MODEL

Following the concept of AP, which is used for characterizing the activation probability of a user, the WFN can be modelled.

TABLE I
LIST OF SYMBOLS

Symbol	Definition
c_u	The u-th CU
$\{d_x, d_{m(x)}\}$	The x-th D2D pair
G_i	The traffic density of i-th user
$\mathbb{P}[\tau]$	The probability that a user generate τ packets in a period
$\mathbb{P}_i$	The probability that i-th user is activated in a time slot
Φ_b	PPP to constitute BSs
Φ_c	PPP to constitute CUs
Φ_d	PPP to constitute DUs
$\mathcal{P}_i$	The transmit power of i-th user
$\mathcal{P}_{i2j}$	The received power at j transmitted by i
g_{i2j}	The channel fading coefficient between i and j
D_{i2j}	The distant between i and j
α	The standard path loss exponent
h_{i2j}	The channel gain between i and j
$\boldsymbol{H}$	The channel gain matrix formed by h_{ij}
$\bar{\boldsymbol{H}}$	The normalized channel gain matrix
R	The maximum cellular link distance
R_d	The maximum D2D link distance
μ	The self-interference cancellation coefficient
σ^2	The noise power
N_c	The number of CUs in a BS-centered cell
N_d	The number of DUs in a BS-centered cell
N	The total number of users in a BS-centered cell
N_{input}	The number of elements at the input layer
N_{HL}	The number of sub-blocks at the hidden layer
N_{output}	The number of elements at the output layer
F_k	The number of neurons for the k-th sub-block
D	The number of drop-outed neurons
ϵ	The SINR threshold
η_i	The PSS weight of i-th user
η_s	The SINR constraints weight
θ_i	The validation coefficient of i-th user
$\hat{\boldsymbol{O}}$	The inputs vector of proposed DNN
$\hat{\boldsymbol{V}}$	The weights matrix of proposed DNN
$\hat{\boldsymbol{b}}$	The biases vector of proposed DNN

A. Activated Probability

To analysis the performance of WFN under variant traffic densities, some hypotheses should be made firstly. Following the Poisson distribution, the probability that a user (either a CU or a DU) generates τ consecutive packets (i.e., source data) during a given period can be expressed:

$$\mathbb{P}[\tau] = \frac{G^\tau e^{-G}}{\tau!} \tag{1}$$

where G denotes the average traffic density. Therefore, the probability of "no traffic is generated" can be denoted by e^{-G}. In practice, if a user has data to transmission, it should not switch to "inactivation" state until the pending data is completely transmitted. In this sense, AP can be used to characterize a user's workload. The probabilities that a CU (the u-th CU, for example) and a DU (the x-th DU, for example) are activated can thus be expressed as $\mathbb{P}_{c_u} = 1 - e^{-G_{c_u}}$ and $\mathbb{P}_{d_x} = 1 - e^{-G_{d_x}}$, respectively, where G_{c_u} and G_{d_x} denote the traffic densities of the u-th CU and the x-th DU, respectively.

B. System Model for FD-D2D-Aided Underlaying CN

According to the existing standards such as ProSe [46], the pre-allocated uplink licensed spectrum for the CNs is also allowed to be reused by the D2D links in the FN. Therefore, interference happens in the uplink, which will be focused by this paper.

In this reuse-spectrum scenario, devices such as the BSs, N_c CUs and N_d D2D pairs are assumed to be randomly distributed within a given area according to non-homogeneous PPP models Φ_b, Φ_c and Φ_d, respectively, enabling a maximum CU-to-BS distance of R. Meanwhile, the maximum distance between D2D pairs is assumed to be R_d. Without loss of generality, the network is assumed to be capable of offering services to a group of users (comprising both CUs and DUs) simultaneously. In particular, if a given DU is marked as $d_x \in \Phi_d$, its peer would be marked as $d_{m(x)}$, in which case both $m[m(x)] = x$ and $\max(\| d_x - d_{m(x)} \|) = R_d$ can be satisfied.

Denote by $\mathcal{P}_{i2j}$ the signal power received at user j that was transmitted by user i, we get

$$\mathcal{P}_{i2j} = \mathcal{P}_i g_{i2j} D_{i2j}^{-\alpha} = \mathcal{P}_i h_{i2j} \tag{2}$$

where $\mathcal{P}_i$ represents the transmit power of user i, while $g_{i2j} \frown \exp(1)$ denotes the (exponentially distributed) channel fading coefficient between the transmitter i and the receiver j. Furthermore, D_{i2j} stands for the distance between transmitter i and receiver j. In addition, h_{ij} instead of $g_{i2j} D_{i2j}^{-\alpha}$ is used to denote the channel gain.

In particular, the average power of thermal noise is assumed to be σ^2, and the average RSI power of the x-th DU can be given by $I_{d_x}^{\mathrm{RSI}} = \mathcal{P}_{d_x}/\mu$, where μ denotes the SIC coefficient.[1] Furthermore, α is used to express the standard path-loss exponent subjecting to a constraint $\alpha > 2$. In addition, each wireless link

[1]We assume that the SI has been suppressed by using an appropriate SIC technique, in which a higher SIC coefficient corresponds to a higher SI cancellation capability.
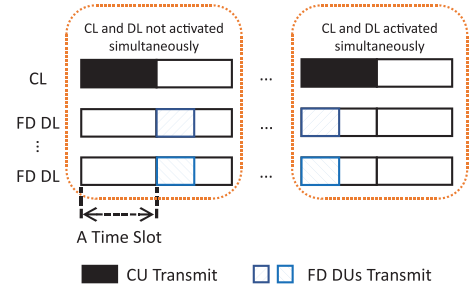

Fig. 1. The transmission scenarios.

is assumed to be independent and identically distributed (i.i.d.) random variable that follows the above-mentioned model.

C. Penalty Based Data Rate of a Typical Link

If the received SINR of a typical link reaches its predetermined threshold ϵ, we consider this transmission as successful, which reflects the quality of this link in the current transmission. Otherwise, if an unsuccessful transmission occurs, the transmission shall not stop retransmission until the current data is received successfully by the receiver.

To express the link gain or distortion caused by Successful-or-Unsuccessful-Transmit (SUT), a penalty coefficient (PC) is introduced in the received SINR expression to represent the performance loss caused by the unsuccessful transmission. Therefore, the received SINR of a randomly chosen user (either a CU or a DU, marked as ∘) with PC can be represented:

$$\mathrm{SINR}_\circ^\dagger = \begin{cases} \mathrm{SINR}_\circ & \text{for } \mathrm{SINR}_\circ \geq \epsilon \text{ or } \mathrm{SINR}_\circ = 0 \\ -\varrho_\circ & \text{for } 0 < \mathrm{SINR}_\circ < \epsilon \end{cases} \tag{3}$$

where the positive real number $\varrho_\circ$ denotes the proposed PC of this user. Based on the above-equation, the penalty-based data-rate (PD) of a user (marked as ∘) can be derived:

$$\mathcal{R}_\circ^\dagger = \log_2(1 + \mathrm{SINR}_\circ^\dagger) \tag{4}$$

Basically, whenever an unsuccessful transmit occurs, the retransmission operation inevitably squeezing the spectrum resources that the subsequent data should obtain, resulting in a decrease in sum data rate. In other words, the sum data rate of WFN depends not only on the received SINR of the link, but also on the probability of successful transmission of an individual packet. In the following, we will use PD to reflect the severity of performance degradation caused by each user's unsuccessful transmission.

III. RECEIVED SINR AT CELLULAR/D2D LINKS IN WORKLOAD DRIVEN NETWORKS

Within each time slot, the D2D links (DLs) would have an opportunity to be activated (as requested), provided that a tolerable performance must be guaranteed at the co-spectrum cellular links (CLs). Basically, we have two choices[2] for the activation of each data-interaction link, as shown in Fig. 1:

[2]We assume that the CUs have the same amount of traffic as the D2D pairs.

1) The co-spectrum CLs and DLs are allowed to be activated simultaneously in a given time slot;

2) The co-spectrum CLs and DLs are not allowed to be activated simultaneously in any time slot. Whenever the CLs are activated, their co-spectrum DLs must remain silence, and vice versa. However, if the users applying to be activated fall into the same category (either all-CLs or all-DLs), they are definitely allowed to be activated simultaneously, because the simultaneous activation will cause no cross-interference between CLs and their co-spectrum DLs in this case.

In practical scenarios, considering that all users are randomly distributed within the cell by following Poisson distribution in their traffic density (as shown in (1)), each user is allowed to be independently activated according to the respective service-arrival time.

A. Co-Spectrum CLs and DLs are Allowed to be Activated Simultaneously

For a given activated CL or DL, it suffers an interference from the other DLs/CLs. The received SINR (i.e., associated with signal received by the BS (from the u-th CU) or the x-th DU) can be expressed:

$$\text{SINR}^{\star}_{c_u} = \frac{\mathcal{P}_{c_u 2b}}{I_{cc} + I_{dc} + \sigma^2} \qquad (5)$$

and

$$\text{SINR}^{\star}_{d_x} = \frac{\mathcal{P}_{d_{m(x)} 2 d_x}}{I_{cd} + I_{dd} + \sigma^2 + I^{\text{RSI}}_{d_x}} \qquad (6)$$

respectively, where the expected inter-CU-interference can be given by $I_{cc} = \sum_{c_v \in \Phi_c / c_u} \mathbb{P}_{c_v} \mathcal{P}_{c_v 2b}$, with c_u and c_v denoting the u-th and v-th CU within Φ_c, respectively. Furthermore, $\mathbb{P}_{c_v}$ is used to denote the AP of the v-th CU that embodies the amount of this CU's workload. We must emphasize that the inter-CU-interference I_{cc}, a statistical variable, can be used to reflect the influence intensity that caused by the workload of each user. In other words, the heavier the workload, the higher the AP of a CU, implying that the high-AP CU can contribute more to the inter-CU-interference. Following this statistical interference expression, the interference imposed on the CUs by its co-spectrum DUs can be denoted by $I_{dc} = \sum_{d_y \in \Phi_d} \mathbb{P}_{d_y} \mathcal{P}_{d_y 2b}$, where $\mathbb{P}_{d_y}$ represents the AP of the y-th DU. Furthermore, we use $I_{cd} = \sum_{c_v \in \Phi_c} \mathbb{P}_{c_v} \mathcal{P}_{c_v 2d}$ to represent the interference imposed on the DUs by their co-spectrum CUs. In addition, $I_{dd} = \sum_{d_y \in \Phi_d / \{d_x, d_{m(x)}\}} \mathbb{P}_{d_y} \mathcal{P}_{d_y 2 d_x}$ is used to represent the interference among the activating DUs. Finally, the average RSI power of the x-th DU can be expressed as $I^{\text{RSI}}_{d_x} = \mathcal{P}_{d_x} / \mu$. In the following, we will use the SIC coefficient μ instead of I^{RSI}_i to denote the RSI power of i-th user.

B. Co-Spectrum CLs and DLs are Not Allowed to be Activated Simultaneously

In this case, there exists no cross-interference between CUs and DUs. In the sequel, the received SINR conceived by the BS

(from the u-th CU) or the x-th DU can be expressed:

$$\text{SINR}^{\diamond}_{c_u} = \frac{\mathcal{P}_{c_u 2b}}{I_{cc} + \sigma^2} \qquad (7)$$

and

$$\text{SINR}^{\diamond}_{d_x} = \frac{\mathcal{P}_{d_{m(x)} 2 d_x}}{I_{dd} + \sigma^2 + I^{\text{RSI}}_{d_x}} \qquad (8)$$

respectively.

IV. PENALTY BASED SUM DATE RATE OF D2D-AIDED UNDERLAYING NETWORK

A. Workload Driven Received Statistical SINR

To simplify the system model, by combining (5) - (8), the received SINR of the i-th user can be rewritten as

$$\text{SINR}_i = \frac{\mathcal{P}_{m(i)} h_{m(i) 2i}}{\sum_{j \neq i, m(i)} \mathbb{P}_j \mathcal{P}_j h_{j 2i} + \sigma^2 + \frac{\theta_i \mathbb{P}_i \mathcal{P}_i}{\mu}} \qquad (9)$$

If user i is a CU, both $i = m(i)$ and $h_{m(i) 2i} = h_{i 2b}$ can be satisfied; otherwise, $\{i, m(i)\}$ denotes a typical D2D pair and satisfies $m[m(i)] = i$. Furthermore, θ_i is a validation coefficient of i-th user, which is set to be 0 for CUs and 1 for DUs. In addition, $\mathbb{P}_{\circ}$ denotes the AP of user $\circ$. Obviously, (9) covers both scenarios shown in Section III. Similar to (3), the penalty-based received statistical SINR of user i (denoted as $\text{SINR}^{\dagger}_i$) can be derived.

B. Penalty Based Statistical Sum Date Rate of WFN

Based on the received SINR at CLs/DLs as well as the PD of a user shown in (4), the penalty-based statistical sum-data-rate (PSS) in the WFN can be given:

$$\mathcal{R}^{\dagger} = W \sum_i \mathbb{P}_i \mathcal{R}^{\dagger}_i = W \sum_i \mathbb{P}_i \log_2(1 + \text{SINR}^{\dagger}_i) \qquad (10)$$

where $\mathbb{P}_i$ denotes the AP of the i-th user, and W represents the bandwidth. It should be emphasized that we have introduced $\mathbb{P}_i$ as the weighted coefficient of the i-th user's PSS to reflect the influence imposed on the statistical performance of the whole networks by the workload. By combining (3) and (9) - (10), we can explain the role of the PC: when the received SINR at a CL (or a DL) reaches the threshold ϵ, the current transmission contributes positively to the sum data rate; otherwise, a retransmission on an unsuccessfully transmitted packet will be triggered, causing a negative contribution to the sum data rate.

Obviously, we can use the indicator PSS to reflect the impact of workload on the performance of WFN: on the one hand, a user with a heavier workload can contribute more to the sum data rate; on the other hand, a user with a heavier workload will definitely impose a stronger interference on its neighbors (particularly on its co-spectrum users), thus eroding the performance of the WFN.

C. Optimization Function for Power Control

In this part, our goal is to maximum the PSS of each user by optimizing the transmit power under consideration of its

workload. In order to achieve the above objectives, the following optimization problem must be solved:

$$\max_{\{\mathcal{P}_1 \cdots \mathcal{P}_N\}} W \sum_{i \in \{\Phi_c, \Phi_d\}} \mathbb{P}_i \log_2(1 + \text{SINR}_i^\dagger) \tag{11}$$

$$\text{s.t.} \quad 0 \leq \mathcal{P}_i \leq \mathcal{P}_{i-\max}$$

where $\mathcal{P}_{i-\max}$ denotes the maximum transmit power of the i-th user.

It should be emphasized that the optimal problem shown in (11) is an NP-hard non-convex optimization, which is hard to address, if not impossible [41]. To address this issue, both the sub-optimal iterative algorithm and the DNN model are often adopted for solving the non-convex optimization problems.

V. IMPROVED SUBSPACE PURSUIT FOR WFN

To obtain a good solution to the optimization problem shown in (11), a series of iterative algorithms such as SP are often developed. The SP algorithms can be expressed as $s^{t+1} = f^t(s^t; x)$, where both t and $(t+1)$ denote the iterative counters, x is the problem data, and f^t represents a kind of mapping functions to transform the data x and the previous iterative result s^t to the new iterative result s^{t+1}.

A typical SP algorithm is WMMSE, which converts the sum rate maximization problem into a higher dimensional space for solving the well-know MMSE-SINR equality [42]. However, it is usually employed in the HD-D2D network by ignoring the impact of the SI. In the following, we introduce an improved WMMSE-based iterative SP algorithm for the WFN.

Similar to [42], the optimal problem shown in (11) is equivalent to the following workload driven mean squared error (MSE) minimization problem:

$$\min_{\{w_i, u_i, \mathcal{P}_i\}} \sum_{i=1}^{N} \mathbb{P}_i \left(w_i e_i - \log_2(w_i)\right) \tag{12}$$

$$s.t. \quad 0 \leq \mathcal{P}_i \leq \mathcal{P}_{i-\max}$$

where the optimization variables e_i and w_i are both real numbers. Furthermore, the variable e_i can be defined:

$$e_i = \left(1 - u_i \sqrt{\mathcal{P}_{m(i)} h_{m(i)2i}}\right)^2 + u_i^2 \left(\sigma^2 + \frac{\theta \mathbb{P}_i \mathcal{P}_i}{\mu}\right)$$

$$+ \sum_{j \neq i, m(i)} (u_i \sqrt{\mathbb{P}_j \mathcal{P}_j h_{j2i}})^2 \tag{13}$$

The proof of the equivalence between (11) and (12) is elaborated on in Appendix A. Based on the iterative equation-solving process, the sub-optimal values of both u_i and w_i can be derived. After that, the sub-optimal transmit power of the i-th user can be formulated:

$$\mathcal{P}_i^{\text{sub-opt}} = \left(\frac{\mathbb{P}_i u_{m(i)} \sqrt{h_{m(i)2i}}}{\mathbb{P}_{m(i)} w_i u_i^2 \frac{\theta_i}{\mu} + \sum_{j \neq i, m(i)} \mathbb{P}_{m(j)} w_j u_j^2 \mathbb{P}_i h_{i2j}}\right)^2 \tag{14}$$

The proof of (14) is shown in Appendix B. Clearly, while solving the optimization problem (12), the block-coordinate descent method should be employed, in which one set of variables are

Input
1. The channel information between all users: $h_{m(i)2i}, i \in \{\Phi_c, \Phi_d\}$
2. The workload of all users (measured by AP): $\mathbb{P}_i, i \in \{\Phi_c, \Phi_d\}$
Initialization
3. Setup the initial transmit power of each user: $\mathcal{P}_i^0 = \mathcal{P}_{i-\max}$
4. Initialize the iterative counter: $t = 0$;
Iteration
Repeat
5. Update the iterative variable u_i^t:
$u_i^t = \dfrac{\sqrt{\mathcal{P}_i^t h_{m(i)2i}}}{\mathcal{P}_{m(i)} h_{m(i)2i} + \sum_{j \neq i, m(i)} \mathbb{P}_j \mathcal{P}_j^t h_{j2i} + \sigma^2 + \frac{\theta \mathbb{P}_i \mathcal{P}_i^t}{\mu}}$
6. Update the iterative variable w_i^t:
$w_i^t = \frac{1}{1 - u_i^t \sqrt{\mathcal{P}_{m(i)} h_{m(i)2i}}}$
7. Update the transmitting power:
$\mathcal{P}_i^t = \left(\dfrac{\mathbb{P}_i u_{m(i)}^t \sqrt{h_{m(i)2i}}}{\mathbb{P}_{m(i)} w_i^t (u_i^t)^2 \frac{\theta_i}{\mu} + \sum_{j \neq i, m(i)} \mathbb{P}_{m(j)} w_j^t (u_j^t)^2 \mathbb{P}_i h_{i2j}}\right)^2$
8. Update the iterative counter: $t = t + 1$
Until:
$\|\sum_{i \in \{\Phi_c, \Phi_d\}} \log(w_i^t) - \sum_{i \in \{\Phi_c, \Phi_d\}} \log_2(w_i^{t-1})\| < 0.01$
Output
9. Output the optimal transmitting power: $\mathcal{P}_i^{\text{opt}} = \mathcal{P}_i^t$

optimized in each time by keeping the rest to be fixed [47]. Furthermore, according to (14), it should be noticed that the optimization of transmit power is determined by both u_i and w_i, which can be trended to the globally optimal solution by using an iterative process. Therefore, the detailed equation-solving process of this workload-driven improved-iterative SP-algorithm (WIS) is shown in Table II.

VI. DEEP LEARNING BASED TRANSMIT POWER ALLOCATION UNDER SINR CONSTRAINTS

In this section, we propose a new TPA scheme based on DNN structure by giving out a detailed explanation on the structure of the DNN model that can be employed for solving the optimization problem formulated in (11). Furthermore, the detailed procedure of the proposed scheme is also presented.

A. Structure of DNN

In the proposed scheme, the optimized transmit power that formulated in (11) can be attained relying on the DNN model, as illustrated in Fig. 2. Basically, the DNN model comprises three layers, i.e., the input layer, the hidden layer and the output layer. In the following, we will introduce these layers one by one.

1) The Input Layer: The input layer is formed by the channel gain matrix $\boldsymbol{H}$, which can be further sub-divided into four parts:
- The channel gain vector between CUs and BS, which has N_c elements;
- The channel gain vector between DUs and BS, which contains $2N_d$ elements;
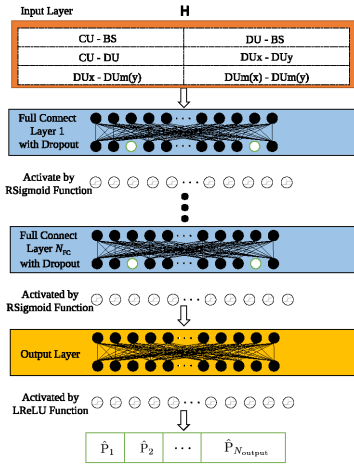- The channel gain matrix between CUs and DUs, which comprises $2N_c N_d$ elements;

Fig. 2.   The DNN structure for optimizing the power allocation.

- The channel gain matrix among DUs, whose elements satisfy $h_{i2j} = h_{j2i}$ for $i, j \in [1, 2N_d]$. There are totally $4N_d^2$ elements in this matrix.

By normalizing the channel gain:

$$\hat{h}_{i2j} = \frac{\log(h_{i2j}) - \mathbb{E}\left[\log(h_{i2j})\right]}{\sqrt{\mathbb{E}\left[\left(\log(h_{i2j}) - \mathbb{E}\left[\log(h_{i2j})\right]\right)^2\right]}} \tag{15}$$

where $\hat{h}_{i2j}$ denotes the normalized channel gain of h_{i2j} in matrix H, for which the normalized channel gain matrix $\hat{H}$ can be reshaped into a one-dimensional vector with a length of $N_{\text{input}} = N_c + 2N_d(1 + N_c + 2N_d)$. After that, the normalized channel gain matrix will be led into the hidden layers.

2) The Hidden Layer: The hidden layer of the proposed DNN model comprises N_{HL} sub-blocks that are connected serially. We must emphasize that each sub-block comprises a fully connected (FC) layer[3] with drop-out and an active layer. In the FC layer, the vector multiplication of the weights is performed, together with the addition of biases. Without loss of generality, the number of neurons for the k-th sub-block is set to be F_k in this paper. Furthermore, a more popular method of setting up F_k is to make all sub-blocks have an identical number of neurons, which is equal to an integer times of N_{input} (called fixed-big-net (FBN). It can be calculated as $F_k = n_1 N_{\text{input}}$). Meanwhile, we propose a method called dynamic-decreasing-net (DDN), in which the number of sub-blocks in the hidden layer can be derived as $N_{\text{HL}} = \lfloor \log_2(n_2 N_{\text{input}}) - \log_2(N_{\text{output}}) - 1 \rfloor$, while the number of neurons in each sub-block can be formulated as $F_k = N_{\text{input}}/2^k$ with $k = 1, \ldots, N_{\text{HL}}$. In addition, by letting O_k, V_k, and b_k denote the inputs vector, weights matrix, and biases vector of the FC layer in the k-th sub-block, respectively, the output of the k-th FC layer becomes

$$\tilde{O}_k = O_k V_k + b_k. \tag{16}$$

Note that every hidden neurons of the FC layer has a connection with the hidden neurons of the previous and the next layers,

[3]Although we have considered a simple FC layer in this article, more complicated layer such as convolution layer is also applicable.

in which manner the FC layer has an ability to mix all input data to extract meaningful features that can be used to determine the transmit power of this user. Meanwhile, several randomly chosen drop-out neurons are adopted in the FC layer to prevent the proposed DNN from over-fitting. The number of drop-out neurons is controlled by the parameter D, which represents the ratio of drop-out-neurons-number to FC-layer-neurons-number.

The output of the k-th FC layer then feeds into an active layer, resulting in non-linearity for a special area of the DNN, where the rectified Sigmoid (RSigmoid) function can be adopted as the active function. In particular, denoting by $\tilde{O}_k$ the input of the k-th RSigmoid layer, the output of RSigmoid layer can be expressed:

$$O_{k+1} = \begin{cases} \tilde{O}_k & \text{for } \tilde{O}_k > 5 \\ 2S(\tilde{O}_k) - 1 & \text{for } \tilde{O}_k \in [0, 5] \\ 0.25\tilde{O}_k & \text{for } \tilde{O}_k < 0 \end{cases} \tag{17}$$

where O_{k+1} represents the input of the $(k+1)$-th FC layer, and $S(x) = 1/(1 + e^{-x})$ is the Sigmoid function. It should be noted that RSigmoid has been used as an activation function, which can mitigate the appearance of vanishing gradient in a BP algorithm.

3) The Output Layer: The last sub-block of hidden layer is also categorized as the output layer, whose output feeds into the limited rectified linear unit (LReLU). Therefore, the final output of LReLU is the vector of transmit power that comprises N_{ouput} elements, as denoted by a vector $\mathcal{P}$ that can be formulated:

$$\mathcal{P} = \min\left[\text{ReLU}(O_{N_{\text{HL}}}), \mathcal{P}_{\max}\right] \tag{18}$$

where $\mathcal{P}_{\max}$ denotes the vector of maximum transmit power. The rectified linear unit (ReLU) function is defined as $\text{ReLU}(x) = \max(0, x)$.

B. Cost Function Design

In this part, we describe the way of designing the cost function of the proposed optimization problem, which makes it possible to maximize the PSS of a cell under certain constraints. To propose a practical mechanism, we should apply the following two constraints to the cost function: i) transmit power constraints, ii) received SINR constraints, in which the former has already been constrained by (18). In the following, we will mainly focus on the latter.

The most typical cost function in deep learning of regression problem is the MSE function, which is an average of square of difference between the predictions and the pre-defined values. To reduce the differences, it usually intends to give benefit or penalty to update DNN. In other words, the cost function can be customized if it can define an appropriate benefit or penalty based on the system's purpose. Therefore, we employ the PSS to act as the cost function for the proposed scheme, as shown in (10). Although the PSS of the actual system is a very complex function, it does not constitute a big trouble to the development of deep learning algorithms. Furthermore, in the proposed scheme, the SINR constraints are also employed in defining the cost function.

In this paper, we adopt the Lagrange function to express the SINR constraints in the cost function. Typically, the Lagrange function can be used to minimize or maximize the cost function (or target value) under certain constraints [48]. Firstly, the SINR constraints, which will be denoted by Γ in the following, are given out:

$$\Gamma = \sum_{i=1}^{N} W \log_2 \left[1 + \frac{\text{ReLU} \left(\epsilon - \text{SINR}_i \right)}{\epsilon} \right] \quad (19)$$

where the ReLU function is employed. If the received SINR of both CLs and DLs can reach the threshold (ϵ), Γ would approach 0. Therefore, only penalty will be delivered if the received SINR of CL or DL is below the constraint. Other than that, the remaining part is designed for re-scaling. If the difference scales between the objective functions (which are PSS in the proposed scheme), and meanwhile the constraints are relatively higher than required, it would be difficult to design the appropriate TPA scheme. Thus, both the objective function and constraints should be designed based on similar scales that have similar forms. Note that the data rate without quantitative unit can be formed by $\log_2(1 + \text{SINR})$. Therefore, the constraints are also designed in terms of data rate $\log_2(1 + \text{ratio})$, in which no quantitative unit is observed in the ratio. Since the proposed design can appropriately re-scale the SINR constraints, it is shown to work effectively in Section VII.

Finally, the cost function of the proposed method can be described as:

$$L = - \sum_{i=1}^{N} \eta_i \mathbb{P}_i \mathcal{R}_i + \eta_s \Gamma \quad (20)$$

where $0 < \eta_i, \eta_s < 1$ denote the weights of the sum data rate for i-th user and the SINR constraints, respectively. Meanwhile, it can also be used to prioritize the transmission of different DUs, i.e., the data rate of x-th DU with a higher η_x value will play a more critical role in the transmit power control. Furthermore, η_s can be derived to adjust the scale of the constraints for further ensuring the optimal scheme. Generally speaking, by proposing this cost function, the optimal problem shown in (11) can be converted to the minimization of cost function L.

C. Training and Inference of the Proposed DNN

In order to implement the proposed scheme, the DNN model must be trained firstly, following which the trained model can be used to determine the transmit power of both CUs and DUs. In the proposed DNN, samples containing channel information that forms a matrix $\boldsymbol{H}$ must be collected. Since information of both the transmitters/receivers' locations and the channel fading coefficients are variant from sample to sample, the optimal transmit power should be channel dependent. Accordingly, the DNN can be trained in arbitrary channel conditions such that a general strategy of transmit power control can be designed. It is worth noting that in our proposed scheme, only the channel sample information is needed without assigning the optimal transmit power to each channel sample, because the optimal

transmit power can be obtained automatically through algorithm training and learning.

A sufficient number of channel samples under various conditions is essentially required for both preventing over-fitting of the training and achieving a high performance (as shown later in the performance evaluation). Furthermore, the collected channel gain should be converted to decibel format and then normalized to have zero mean and unit variance. This preprocessing of data is essential for a proper training, because the characteristics of both path loss and multipath fading imply that the channel gain for different samples may vary significantly, thus adversely affecting the training quality of the DNN.

To implement the proposed scheme, the DNN can be trained by using the stochastic gradient descent (SGD) algorithm [49], in which the weights and biases of the DNN (i.e., in the k-th FC layer, $\boldsymbol{V}_k$ and $\boldsymbol{b}_k$) can be updated as:

$$\begin{cases} \boldsymbol{V}_k^l = \boldsymbol{V}_k^{l-1} - \gamma \dfrac{\partial L}{\partial \boldsymbol{V}_k^{l-1}} \\[4mm] \boldsymbol{b}_k^l = \boldsymbol{b}_k^{l-1} - \gamma \dfrac{\partial L}{\partial \boldsymbol{b}_k^{l-1}} \end{cases} \quad (21)$$

respectively, where γ is the learning rate of the SGD, and $\boldsymbol{V}_k^l$ and $\boldsymbol{b}_k^l$ denote the values of $\boldsymbol{V}_k$ and $\boldsymbol{b}_k$ in the l-th iteration of k-th layer, respectively. In (21), the partial derivative can be formulated by addressing the following iterative equations:

$$\begin{cases} \dfrac{\partial L}{\partial \boldsymbol{V}_k^{l-1}} = \triangledown \boldsymbol{L} \boldsymbol{O}_k^{l-1} \displaystyle\prod_{i=k+1}^{F} \boldsymbol{V}_i^{l-1} \boldsymbol{O}_i^{l-1} \times (1 - \boldsymbol{O}_i^{l-1}) \\[4mm] \dfrac{\partial L}{\partial \boldsymbol{b}_k^{l-1}} = \triangledown \boldsymbol{L} \displaystyle\prod_{i=k+1}^{F} \boldsymbol{O}_i^{l-1} \times (1 - \boldsymbol{O}_i^{l-1}) \end{cases} \quad (22)$$

respectively, where $\triangledown \boldsymbol{L}$ represents the gradient of the loss function L. Furthermore, the i-th element of $\triangledown \boldsymbol{L}$, as denoted by $\triangledown L_i$, can be expressed:

$$\triangledown L_i = - \sum_{j=1}^{N} \eta_j \mathbb{P}_j \frac{\partial \mathcal{R}_j}{\partial \hat{\mathbb{P}}_i} + \eta_s \frac{\partial \Gamma}{\partial \hat{\mathbb{P}}_i} \quad (23)$$

where $\partial \mathcal{R}_j / \partial \hat{\mathbb{P}}_i$ can be accessed:

$$\frac{\partial \mathcal{R}_j}{\partial \hat{\mathbb{P}}_i} = \begin{cases} - \dfrac{\eta_{m(i)} \mathbb{P}_{m(i)} \mathcal{P}_{m(i)} h_{m(i)2i} \theta_i}{(1 + \text{SINR}_i) H_i^2 \mu \ln 2} & \text{for } i = j \\[4mm] \dfrac{\eta_i \mathbb{P}_i h_{m(i)2i}}{(1 + \text{SINR}_{m(i)}) H_{m(i)} \ln 2} & \text{for } i = m(j) \\[4mm] \dfrac{\eta_{m(j)} \mathbb{P}_{m(j)} \mathcal{P}_{m(j)} h_{m(j)2j}}{(1 + \text{SINR}_j) H_j^2 \ln 2} \mathbb{P}_i h_{i2j} & \text{for } i \neq \{j, m(j)\} \end{cases} \quad (24)$$

where $H_i = \sum_{j \neq \{i, m(i)\}} \mathbb{P}_j \mathcal{P}_j h_{j2i} + \sigma^2 + \frac{\theta_i \mathbb{P}_i \mathcal{P}_i}{\mu}$. Furthermore, similar to the treatment of this partial function, we can also derive the partial derivative of Γ by substituting (22)-(24) into (21), in which manner both the updated $\boldsymbol{V}$ and $\boldsymbol{b}$ can be given out.

Based on the above operations, the sufficiently trained DNN can be used for performing transmit power control. To determine

the transmit power, the channel gain has to be converted to decibel format and normalized first. After that, it should be fed into the DNN model, which outputs the normalized transmit power. In general, the training process of DNN may take a relatively longer time. Despite of it, the above costs are worth it, because the already-trained DNN infers the transmit power with a negligible computational cost, thus enabling a cost-efficient real-time operation in the proposed scheme.

VII. Numeric Analysis

In this section, the performance of the proposed TPA scheme will be evaluated numerically. In particular, the impact of workload on PSS will be investigated to reveal the affordable traffic volume in FN. Meanwhile, the influence of a variety of critical parameters, including the RSI (μ), the SINR threshold (ϵ), the PC (ϱ) and the number of D2D pairs in a given cell (N_d) will be taken into account.

A. Simulation Setup

We choose a BS-centric environment with radius $R = 300\,\text{m}$ as the simulation scenarios, within which both CUs and DUs are randomly distributed according to the non-homogeneous PPP models. The licensed uplink band that was supposed to be exclusively allocated to a CU is now allowed to be reused by N_d D2D pairs. Without loss of generality, each link is assumed to be an i.i.d. Rayleigh fading channel, with the path-loss exponent α be 3.8 (i.e., corresponding to a typical urban environment). Furthermore, the maximally tolerable distance between D2D pairs is assumed to be 50 m, in which case all the DUs within this experimental area are assumed to have the same amount of workload. Moreover, the value of PC for all users is set to be 0.2, and the SIC coefficient μ is set to be 60 dB[4]. Under the above-mentioned premise, the noise power spectrum density (PSD) is set to be $-175\,\text{dB/Hz}$ with $W = 1\,\text{MHz}$. Meanwhile, a moderate value of the SINR threshold $\epsilon = 5\,\text{dB}$ is adopted. In addition, the learning rate of proposed DNN is set to be 0.0001 and the decay rate is assumed to be 0.9. Finally, the number of channel samples denoted by N_s for training and test number in each round is set to be 5000.

In the following, two DNN structures (i.e., FBN and DDN) with variant number of hidden layers and nodes for FC are considered, where $n_1 = 1$ and $N_{\text{HL}} = 3$ for FBN, while $n_2 = 1$ for DDN. For a fair comparison, the WIS scheme, the equal-transmit-power (ETP)[5] scheme and random-transmit-power (RTP)[6] are also employed as performance benchmarks.

In short, the detailed parameter settings of the proposed simulations are elaborated on in Table III. Unless stated otherwise, we will always use the above parameter settings in subsequent sections.

TABLE III
SIMULATION PARAMETERS OF THE PROPOSED ANALYSIS

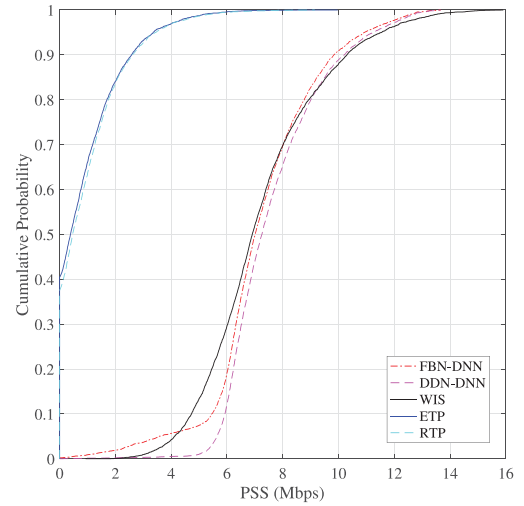| parameters	value
D	0.02
n_1	1
n_2	1
N_c	1
N_d	6
Noise PSD	$-175\,\text{dB/Hz}$
$\mathcal{P}_{\text{c-max}}$	24 dB
$\mathcal{P}_{\text{d-max}}$	20 dB
R	300 m
R_d	50 m
α	3.8
μ	60 dB
ϱ	0.2
ϵ	5 dB
η_1	1
$\eta_i (i > 2)$	0.1
η_s	0.01

Fig. 3. The cumulative distribution function that describes the PSS achieved by different algorithms.

B. The Performance of Proposed Power Allocation Scheme

In this subsection, we assume that the AP of CU and DUs are $\mathbb{P}_c = 0.5$ and $\mathbb{P}_d = \mathbb{P}_c/2$, respectively, in which case both the CU and D2D pairs have the same amount of workload. The cumulative distribution function that describes the PSS achieved by different algorithms is depicted in Fig. 3. It is observed that the PSS performance of the proposed DNN based TPA scheme is very closed to that of the WIS, both significantly outperforming the other two baselines. Furthermore, comparing with FBN-DNN, the DDN-DNN can attain almost the same performance, thus confirming the benefit by implementing DDN-DNN.

C. The Influence Imposed by Workload in WFN

The impact of workload on PSS is plotted in Fig. 4. Without employing a proper TPA scheme, the PSS trend of both the ETP and RTP schemes are described as follows: it firstly increases, then creeps down after passing beyond the break points. We may explain it as follows: the traffic of both CU and DUs are far from

Fig. 4. The PSS-curves derived by different algorithms as function of the workload.
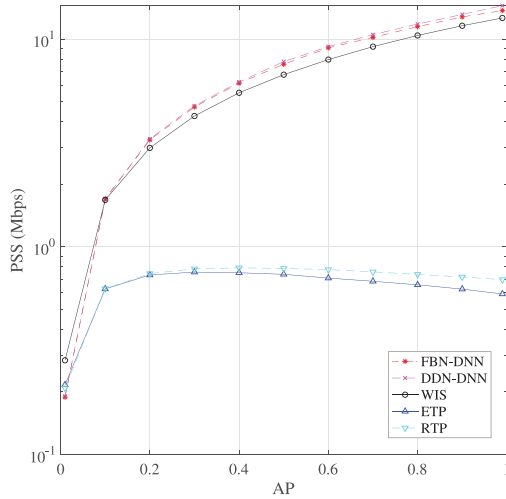

Fig. 5. The PSS-curves derived by different algorithms as function of the number of D2D pairs N_d.

saturation when the number of AP is small, thus making PSS increase rapidly at first. However, the increasing number of AP will cause a severer cross-interference among them, thus eroding the PSS obviously.

On the contrary, by employing a proper TPA scheme in both the proposed scheme and WIS, the PSS will increase along with the increasing of AP. Furthermore, performances of both FBN-DNN and DDN-DNN are very closed to that of the WIS, while DDN-DNN slightly outperforms both WIS and FBN-DNN in high-AP-density scenarios.

When AP is very small (i.e., less than 0.01), it should be emphasized that the proposed DNN based TPA scheme outperforms neither ETP nor RTP. Therefore, optimizing TPA is meaningless in terms of PSS improvement in the presence of a relatively lower traffic in the WFN, because each user can set the maximum transmission power without causing interference between users. Otherwise, when the traffic tends to be saturated, the implementation of un-optimized ETP and RTP schemes will cause a much severer interference.

D. The Influence Imposed by Some Critical Parameters in WFN

In this section, we assume $\mathbb{P}_c = 0.5$ and $\mathbb{P}_d = \mathbb{P}_c/2$ for CUs and DUs, respectively, in which case both the CU and D2D pairs have the same amount of workload. As shown in Fig. 5 – Fig. 8, the performance of the proposed DNN based TPA scheme can be formulated as a function of a variety of parameters, including the number of D2D pairs in a given cell (N_d), the RSI (μ), the SINR threshold (ϵ) and the PC (ϱ), etc.

In Fig. 5, the PSS-curves as functions of the number of D2D pairs (N_d) are described. As N_d increases, the PSS curves of both the ETP and RTP schemes will decrease rapidly due to the impact of the raising MI. However, by using a proper TPA scheme such as the proposed DNN and WIS, the PSS curves will increase at first, followed by a gentler tend. Evidently,
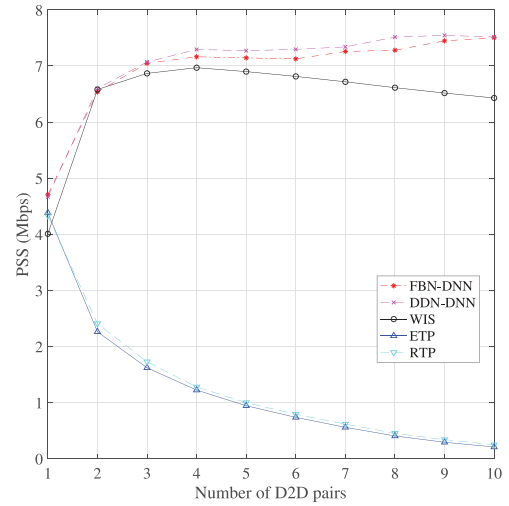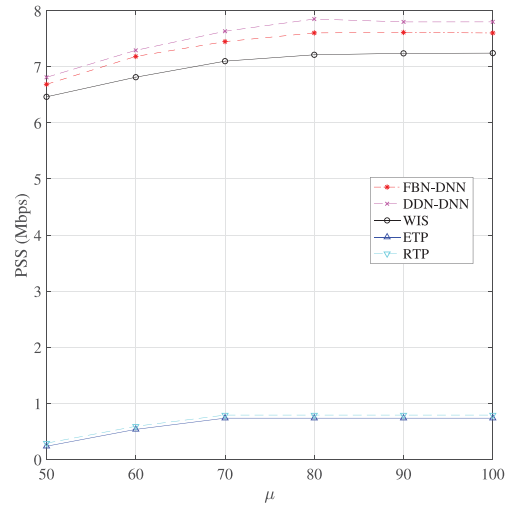

Fig. 6. The PSS-curves derived by different algorithms as function of RSI.
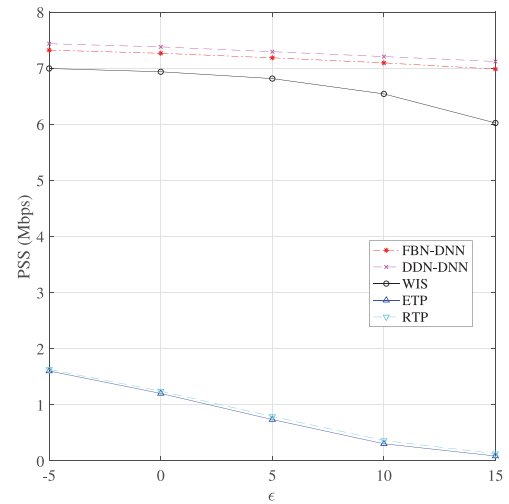

Fig. 7. The PSS-curves derived by different algorithms as function of the SINR threshold ϵ.
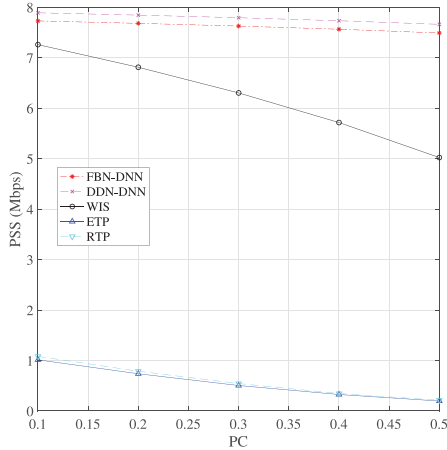
Fig. 8.   The PSS-curves derived by different algorithms as function of penalty coefficent.

Fig. 9.   The computation time curves of FBN-DNN, DDN-DNN and WIS.

the performance of WFN can not be continuously enhanced by simply increasing the D2D pairs. Based on the simulation set-up, the optimal user number is found to be 4, which already leads to a saturated performance. It should be noticed that a slightly performance pacing down occurs for the WIS in the high D2D pair' number scenario, while the PSS of proposed DNN based TPA scheme remains stable. The reason for this observation is that the WIS algorithm ignores the impact of SUT in the iterative process, as considered in the proposed algorithm according to (20), thus imposing extra benefits. Furthermore, the proposed DNN significantly outperforms the other two baselines in the high user-number scenario (i.e., $N_d > 5$), thus confirming the benefit of proposed algorithm. In addition, it is shown that the PSS of DDN-DNN is almost identical to that of BFN-DNN. Therefore, it would be sufficient to employ the DDN-DNN model for optimizing the transmit power.

Note that the average RSI power of DUs can be expressed as $I^{\mathrm{RSI}} = P_d/\mu$, where μ denotes the SIC coefficient. In the following, we will use the μ instead of I^{RSI} to denote the RSI power. In Fig. 6, the PSS-curves derived in variant algorithms as functions of μ are plotted. The PSS of all algorithms are shown to increase as the the SIC capability increases at first, followed by tending to be stable, implying that an unlimited RSI power cancellation process is not necessary. Furthermore, it is still observed that the PSS performance of both proposed DNN and WIS with a proper TPA scheme can be significantly enhanced compare to the other two benchmarks. In addition, the proposed scheme is shown to slightly outperform WIS, which validates the benefit of proposed DNN.

In Fig. 7, the PSS-curves derived by different algorithms as functions of the SINR threshold (ϵ) are plotted. The PSS of all algorithms are shown to reduce as the threshold increases. However, the proposed DNN based TPA is still shown to be stabler than the WIS, enabling the specially designed cost function in (20) to bring about considerable benefits.

In Fig. 8, the PSS-curves of variant algorithms as the function of PC (ϱ) are figured out. The PSS of all algorithms are shown to decline as PC increases, implying that PC can reflect the severity of performance loss when the unsuccessful transmission
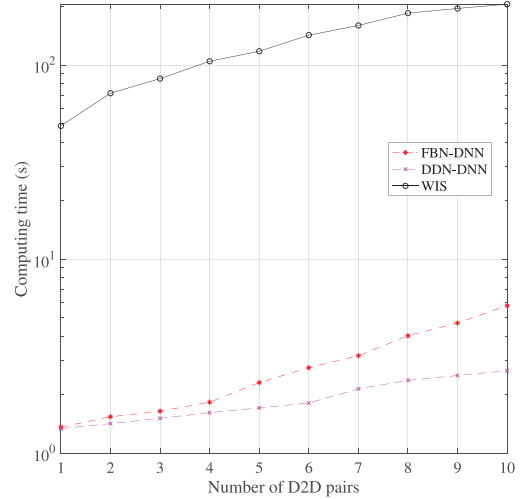
occurs. Furthermore, the proposed DNN based TPA shows a stable performance, while the WIS declines rapidly, confirming the benefits earned by employing the proposed cost function in (20).

E. The Computation Time

In Fig. 9, the time required for calculating the transmit power, depending on the number of the D2D pairs sharing the pre-allocated spectrum with a CU, is described. The computational cost of both the ETP and RTP schemes are absent, because the transmit power calculation is unnecessary in both schemes, corresponding to almost zero cost in terms of computational time. When $N_d = 10$ and $N_s = 5000$, DNN training takes more than 10*min* (although the above information is absent in this article, the above data can still be obtained through our previously simulation). Even so, considering the fact that the training process can be performed in advance, the training overhead will not cause any obstacle to the real-time operation of the proposed scheme.

Simulation results show that the implementing time of all three algorithms will approximately increase exponentially as the number of users increases. However, the operational time of both FBN-DNN and DDN-DNN is much less than that of the WIS, fully validating the priority of the proposed DNN based TPA over the iterative algorithm. In addition, the DDN-DNN cost obviously less computational time than FBN-DNN (while achieving the almost same PSS performance), which confirms the performance advantage of the proposed neuron generating scheme.

VIII. CONCLUSION

In this paper, the performance gains brought about by implementing a deep learning based TPA scheme in WFN were analyzed. The closed-form expressions for the PSS, as the performance metric, were firstly given out by involving the impact of workload. At the same time, we also introduced a new concept of "penalty" (corresponding to the PC) to characterize

"performance loss caused by retransmission of data that has been transmitted but not successfully received (that is, the received SINR does not reach the minimum threshold)". Furthermore, based on the features of WFN, an improved iterative subspace pursuit algorithm for WFN was proposed as the performance benchmark. After that, a TPA scheme was proposed for performing FNs based on deep learning, in which the optimal transmit power (i.e., for maximizing the PSS) can be learned in arbitrary channel conditions by employing the DNN structure. Numerical results showed that the PSS of WFN with extremely workload density can be significantly enhanced by employing proper TPA schemes. Meanwhile, the research results showed that the performance proposed TPA scheme was very closed to the iterative algorithm by costing much less computational time. In addition, it was shown that the eroded PSS of WFN by a variety of critical parameters, including the number of D2D pairs, the RSI, the SINR threshold and the PC, etc, can be tremendously relieved by applying the proposed TPA scheme.

APPENDIX A

Based on (13), a sub-optimal solution of u_i can be derived by calculating the partial derivation of e_i:

$$u_i = \frac{\sqrt{\mathcal{P}_i h_{m(i)2i}}}{\mathcal{P}_{m(i)} h_{m(i)2i} + \sum_{j \neq i, m(i)} \mathbb{P}_j \mathcal{P}_j h_{j2i} + \sigma^2 + \frac{\theta \mathbb{P}_i \mathcal{P}_i}{\mu}} \tag{25}$$

By substituting (25) into (13), we can formulated the sub-optimal solution of e_i:

$$e_i = \frac{\sum_{j \neq i, m(i)} \mathbb{P}_j \mathcal{P}_j h_{j2i} + \sigma^2 + \frac{\theta \mathbb{P}_i \mathcal{P}_i}{\mu}}{\mathcal{P}_{m(i)} h_{m(i)2i} + \sum_{j \neq i, m(i)} \mathbb{P}_j \mathcal{P}_j h_{j2i} + \sigma^2 + \frac{\theta \mathbb{P}_i \mathcal{P}_i}{\mu}} \tag{26}$$

By setting $w_i = e_i^{-1}$, the w_i can be formulated:

$$w_i = \frac{1}{1 - u_i \sqrt{\mathcal{P}_{m(i)} h_{m(i)2i}}} \tag{27}$$

$$= 1 + \text{SINR}_i$$

Furthermore, by plugging both (25) and (27) into (12), a equivalence of problem (12) can be expressed:

$$\min_{\{\mathcal{P}_i\}_{i=1}^N} \sum_{i=1}^N \mathbb{P}_i \left[1 - \log_2(1 + \text{SINR}_i)\right] \tag{28}$$

$$s.t. \quad 0 \leq \mathcal{P}_i \leq \mathcal{P}_{i-\max} \quad i = 1, \ldots, N$$

which is obviously equivalent to (11).

APPENDIX B

According to (11), the cost function for the optimization is $L = \sum_{i=1}^N \mathbb{P}_i \log_2(1 + \text{SINR}_i)$. The partial derivative of L with respect to $\sqrt{\mathcal{P}_i}$ can be formulated:

$$\frac{\partial L}{\partial \sqrt{\mathcal{P}_i}} = \frac{2\mathbb{P}_i \sqrt{\mathcal{P}_{m(i)} h_{m(i)2i}}}{w_{m(i)} H_{m(i)} \ln 2} - \frac{2\mathbb{P}_{m(i)} \mathcal{P}_{m(i)} h_{m(i)2i} \theta_i \sqrt{\mathcal{P}_i}}{w_i H_i^2 \mu \ln 2} \\ - \frac{2}{\ln 2} \sum_{j \neq \{i, m(i)\}} \frac{\mathbb{P}_{m(j)} \mathcal{P}_{m(j)} h_{m(j)2j}}{w_j H_j^2} \mathbb{P}_i \sqrt{\mathcal{P}_i} h_{i2j} \tag{29}$$

where $H_i = \sum_{j \neq \{i, m(i)\}} \mathbb{P}_j \mathcal{P}_j h_{j2i} + \sigma^2 + \frac{\theta \mathbb{P}_i \mathcal{P}_i}{\mu}$. By substituting both (25) and (27) into (29), and setting the partial derivative to zero, the sub-optimal transmitting power shown in (14) can be derived.

REFERENCES

[1] Z. Zhang, K. Long, J. Wang, and F. Dressler, "On swarm intelligence inspired self-organized networking: Its bionic mechanisms, designing principles and optimization approaches," *IEEE Commun. Surv. Tut.*, vol. 16, no. 1, pp. 513–537, Jan.–Mar. 2014.

[2] S. Chen, Q. Fei, H. Bo, L. Xi, and Z. Chen, "User-centric ultra-dense networks for 5G: Challenges, methodologies, and directions," *IEEE Wireless Commun.*, vol. 23, no. 2, pp. 78–85, Apr. 2016.

[3] W. Sun, J. Liu, Y. Yue, and Y. Jiang, "Social-aware incentive mechanisms for D2D resource sharing in IIoT," *IEEE Trans. Ind. Informat.*, vol. 16, no. 8, pp. 5517–5526, Aug. 2020.

[4] Z. Zhang, K. Long, and J. Wang, "Self-organization paradigms and optimization approaches for cognitive radio technologies: A survey," *IEEE Wireless Commun.*, vol. 20, no. 2, pp. 36–42, Apr. 2013.

[5] K. Chi, L. Huang, Y. Li, Y. Zhu, X. Tian, and M. Xia, "Efficient and reliable multicast using device-to-device communication and network coding for a 5G network," *IEEE Netw.*, vol. 31, no. 4, pp. 78–84, Jul.–Aug. 2017.

[6] C. Xing, M. Ying, Y. Zhou, and F. Gao, "Transceiver optimization for multi-hop communications with per-antenna power constraints," *IEEE Trans. Signal Process.*, vol. 64, no. 6, pp. 1519–1534, Mar. 2016.

[7] K. Yang, N. Yang, N. Ye, M. Jia, Z. Gas, and R. Fan, "Non-orthogonal multiple access: Achieving sustainable future radio access," *IEEE Commun. Mag.*, vol. 57, no. 2, pp. 116–121, Feb. 2019.

[8] J. An, K. Yang, J. Wu, N. Ye, S. Guo, and Z. Liao, "Achieving sustainable ultra-dense heterogeneous networks for 5G," *IEEE Commun. Mag.*, vol. 55, no. 12, pp. 84–90, Dec. 2017.

[9] Z. Liu, P. Tao, P. Bo, and W. Wang, "Sum-capacity of D2D and cellular hybrid networks over cooperation and non-cooperation," in *Proc. Int. 7th Conf. Commun. Netw. China*, 2012, pp. 707–711.

[10] A. A. A. Haija and V. Mai, "Spectral efficiency and outage performance for hybrid D2D-infrastructure uplink cooperation," *IEEE Trans. Wireless Commun.*, vol. 14, no. 3, pp. 1183–1198, Mar. 2015.

[11] C. Xu, P. Zeng, W. Liang, and H. Yu, "Secure resource allocation for green and cognitive device-to-device communication," *Sci. China Inf. Sci.*, vol. 61, no. 2, pp. 1–3, Feb. 2018.

[12] J. Liu, S. Zhang, H. Nishiyama, N. Kato, and J. Guo, "A stochastic geometry analysis of D2D overlaying multi-channel downlink cellular networks," in *Proc. IEEE Conf. Comput. Commun.*, 2015, pp. 46–54.

[13] G. Fodor *et al.*, "Design aspects of network assisted device-to-device communications," *IEEE Commun. Mag.*, vol. 50, no. 3, pp. 170–177, Mar. 2012.

[14] R. Zhang, Y. Li, C.-X. Wang, Y. Ruan, and H. Zhang, "Energy efficient power allocation for underlaying mobile D2D communications with peak/average interference constraints," *Sci. China Inf. Sci.*, vol. 61, no. 8, pp. 221–223, Aug. 2018.

[15] L. Lei, Y. Kuang, X. Shen, C. Lin, and Z. Zhong, "Resource control in network assisted device-to-device communications: Solutions and challenges," *IEEE Commun. Mag.*, vol. 52, no. 6, pp. 108–117, Jun. 2014.

[16] Z. Zhang, K. Long, A. V. Vasilakos, and L. Hanzo, "Full-duplex wireless communications: Challenges, solutions, and future research directions," in *Proc. IEEE*, vol. 104, no. 7, pp. 1369–1409, Jul. 2016.

[17] Z. Zhang, X. Chai, K. Long, and A. V. Vasilakos, "Full duplex techniques for 5G networks: Self-interference cancellation, protocol design, and relay selection," *IEEE Commun. Mag.*, vol. 53, no. 5, pp. 128–137, May 2015.

[18] B. Zhong and Z. Zhang, "Opportunistic two-way full-duplex relay selection in underlay cognitive networks," *IEEE Syst. J.*, vol. 12, no. 1, pp. 725–734, Mar. 2018.

[19] H. Min, J. Lee, S. Park, and D. Hong, "Capacity enhancement using an interference limited area for device-to-device uplink underlaying cellular networks," *IEEE Trans. Wireless Commun.*, vol. 10, no. 12, pp. 3995–4000, Dec. 2011.

[20] C. Ma, J. Liu, X. Tian, Y. Hui, C. Ying, and X. Wang, "Interference exploitation in D2D-enabled cellular networks: A secrecy perspective," *IEEE Trans. Commun.*, vol. 63, no. 1, pp. 229–242, Jan. 2015.

[21] C. Du, Z. Zhang, X. Wang, and J. An, "Optimal duplex mode selection for D2D-aided underlaying cellular networks," *IEEE Trans. Veh. Technol.*, vol. 69, no. 3, pp. 3119–3134, Mar. 2020.

[22] W. Li, T. Fei, T. Svensson, D. Feng, and S. Li, "Exploiting full duplex for device-to-device communications in heterogeneous networks," *IEEE Commun. Mag.*, vol. 53, no. 5, pp. 146–152, May 2015.

[23] C. Yang, Q. Cui, J. Han, and X. Tao, "Bipartite matching approach to optimal resource allocation in device to device underlaying cellular network," *Electron. Lett.*, vol. 50, no. 3, pp. 212–214, Jan. 2014.

[24] B. Rong, Z. Zhang, X. Zhao, and X. Yu, "Robust superimposed training designs for MIMO relaying systems under general power constraints," *IEEE Access*, vol. 7, pp. 80 404–80 420, 2019.

[25] N. Lee, X. Lin, J. G. Andrews, and R. W. Heath, "Power control for D2D underlaid cellular networks: Modeling, algorithms, and analysis," *IEEE J. Sel. Areas Commun.*, vol. 33, no. 1, pp. 1–13, Jan. 2015.

[26] Wei Yu, G. Ginis, and J. M. Cioffi, "Distributed multiuser power control for digital subscriber lines," *IEEE J. Sel. Areas Commun.*, vol. 20, no. 5, pp. 1105–1115, Jun. 2002.

[27] D. A. Schmidt, C. Shi, R. A. Berry, M. L. Honig, and W. Utschick, "Distributed resource allocation schemes," *IEEE Signal Process. Mag.*, vol. 26, no. 5, pp. 53–63, Sep. 2009.

[28] Z.-Q. Luo, W.-K. Ma, A. M. So-Cho, Y. Ye, and S. Zhang, "Semidefinite relaxation of quadratic optimization problems," *Signal Process. Mag., IEEE*, vol. 27, no. 3, pp. 20–34, May 2010.

[29] Q. Shi, M. Razaviyayn, Z. Luo, and C. He, "An iteratively weighted MMSE approach to distributed sum-utility maximization for a MIMO interfering broadcast channel," *IEEE Trans. Signal Process.*, vol. 59, no. 9, pp. 4331–4340, Sep. 2011.

[30] Y. Jiang, Q. Liu, F. Zheng, X. Gao, and X. You, "Energy efficient joint resource allocation and power control for D2D communications," *IEEE Trans. Veh. Technol.*, vol. 65, no. 8, pp. 6119–6127, Aug. 2016.

[31] J. Wang, D. Zhu, C. Zhao, J. C. F. Li, and L. Ming, "Resource sharing of underlaying device-to-device and uplink cellular communications," *IEEE Commun. Lett.*, vol. 17, no. 6, pp. 1148–1151, Jun. 2013.

[32] D. Feng, L. Lu, Y. W. Yi, G. Y. Li, G. Feng, and S. Li, "Device-to-device communications underlaying cellular networks," *IEEE Trans. Commun.*, vol. 61, no. 8, pp. 3541–3551, Aug. 2013.

[33] K. Yang, S. Martin, C. Xing, J. Wu, and R. Fan, "Energy-efficient power control for device-to-device communications," *IEEE J. Sel. Areas Commun.*, vol. 34, no. 12, pp. 3208–3220, Dec. 2016.

[34] K. Simonyan and A. Zisserman, "Very deep convolutional networks for large-scale image recognition," 2014, *arXiv:1409.1556*.

[35] T. J. OShea, J. Corgan, and T. C. Clancy, "Convolutional radio modulation recognition networks," in *Int. Conf. Eng. Appl. Neural Netw.*, Sep. 2016, pp. 213–226.

[36] A. Krizhevsky, I. Sutskever, and G. E. Hinton, "ImageNet classification with deep convolutional neural networks," *Commun. ACM*, vol. 60, no. 6, pp. 84–90, May 2017.

[37] H. Ye, G. Y. Li, and B. H. F. Juang, "Power of deep learning for channel estimation and signal detection in OFDM systems," *IEEE Wireless Commun. Lett.*, vol. 7, no. 1, pp. 114–117, Feb. 2018.

[38] Z. Zou, R. Yin, X. Chen, and C. Wu, "Deep reinforcement learning for D2D transmission in unlicensed bands," in *Proc. IEEE/CIC Int. Conf. Commun. Workshops China*, 2019, pp. 42–47.

[39] W. Sun, J. Liu, and Y. Yue, "AI-Enhanced offloading in edge computing: When machine learning meets industrial IoT," *IEEE Netw.*, vol. 33, no. 5, pp. 68–74, Sep.–Oct. 2019.

[40] Z. Li and C. Guo, "Multi-agent deep reinforcement learning based spectrum allocation for D2D underlay communications," *IEEE Trans. Veh. Technol.*, vol. 69, no. 2, pp. 1828–1840, Feb. 2020.

[41] H. Sun, X. Chen, Q. Shi, M. Hong, X. Fu, and N. D. Sidiropoulos, "Learning to optimize: Training deep neural networks for wireless resource management," in *Proc. IEEE Int. Workshop Signal Process. Adv. Wireless Commun.*, 2017, pp. 1–6.

[42] H. Sun, X. Chen, Q. Shi, M. Hong, X. Fu, and N. D. Sidiropoulos, "Learning to optimize: Training deep neural networks for interference management," *IEEE Trans. Signal Process.*, vol. 66, no. 20, pp. 5438–5453, Oct. 2018.

[43] W. Lee, M. Kim, and D. H. Cho, "Deep learning based transmit power control in underlaid device-to-device communication," *IEEE Syst. J.*, vol. 13, no. 3, pp. 2551–2554, Sep. 2019.

[44] F. Liang, C. Shen, W. Yu, and F. Wu, "Towards optimal power control via ensembling deep neural networks," *IEEE Trans. Commun.*, vol. 68, no. 3, pp. 1760–1776, Mar. 2020.

[45] J. Kim, J. Park, J. Noh, and S. Cho, "Completely distributed power allocation using deep neural network for device to device communication underlaying LTE," 2018, *arXiv:1802.02736*.

[46] S. Lien, C. Chien, G. S. Liu, H. Tsai, R. Li, and Y. J. Wang, "Enhanced LTE device-to-device proximity services," *IEEE Commun. Mag.*, vol. 54, no. 12, pp. 174–182, Dec. 2016.

[47] D. P. Bertsekas and J. N. Tsitsiklis, *Parallel and Distributed Computation: Numerical Methods*, vol. 23, Englewood Cliffs, NJ, USA: Prentice-Hall, 1989.

[48] Y. Peng, Y. Hong, and L. Feng, "Distributed gradient algorithm for constrained optimization with application to load sharing in power systems," *Syst. Control Lett.*, vol. 83, no. 711, pp. 45–52, Sep. 2015.

[49] D. P. Kingma and J. Ba, "Adam: A method for stochastic optimization," 2014, *arXiv:1412.6980*.

Changhao Du received the Ph.D. degree from the Beijing Institute of Technology, China, in 2018. From 2016 to 2017, he was a Visiting Ph.D. Student with the Chalmers University of Technology, Sweden, under the financial support of China Scholarship Council. Since 2018, he has been with the Beijing University of Posts and Telecommunications, China, as a Post-doctoral Research Associate. His research interest include statistical signal processing, applied signal processing and physical layer of wireless communication systems, including D2D communications, GPS navigation, laser and THz communications, and channel estimation and synchronization.

Zhongshan Zhang (Senior Member, IEEE) received the B.E. and M.S. degrees in computer science from the Beijing University of Posts and Telecommunications (BUPT), in 1998 and 2001, respectively, and received the Ph.D. degree in electrical engineering in 2004 from BUPT. From 2004, he joined DoCoMo Beijing Laboratories as an Associate Researcher, and was promoted to be a Researcher in 2005. From 2006, he joined the University of Alberta, Edmonton, AB, Canada, as a Postdoctoral Fellow. From 2009, he joined the Department of Research and Innovation (R&I), Alcatel-Lucent, Shanghai, as a Research Scientist. From 2010 to 2011, he was with NEC China Laboratories, as a Senior Researcher. He is currently a Professor of the School of Communication and Electronics with the Beijing Institute of Technology (BIT). His main research interests include statistical signal processing, self-organized networking, cognitive radio, and cooperative communications. He was a Guest Editor and/or an Editor for several technical journals, such as the *IEEE Communications Magazine* and KSII *Transactions on Internet and Information Systems*.

Xiaoxiang Wang received the B.S degree in physics from Qufu Normal University, Qufu, China, in 1991, the M.S. degree in information engineering from East China Normal University, Shanghai, China, in 1994, and the Ph.D. degree in electronic engineering from the Beijing Institute of Technology, Beijing, China, in 1998. In 1998, she joined the School of Information and Communication Engineering, Beijing University of Posts and Telecommunications. From 2010 to 2011, she was a Visiting Fellow with the Department of Electrical and Computer Engineering, North Carolina State University, Raleigh. Her research interests include communications theory and signal processing, with specific interests in cooperative communications, mobile edge computing, multimedia broadcast/multicast service systems, and resource allocation.

Jianping An (Member, IEEE) received the Ph.D. degree from the Beijing Institute of Technology, China, in 1996. He joined the School of Information and Electronics, Beijing Institute of Technology, in 1995, where he is now a Full Professor. He is currently the Dean of the School of Information and Electronics, Beijing Institute of Technology. He has authored or coauthored more than 150 journal and conference articles and holds (or co-holds) more than 50 patents. His research interests include digital signal processing, wireless communications, and satellite networks. He was the recipient of the various awards for his academic achievements and the resultant industrial influences, including two National Awards for technological inventions and science and technology progress.